Organic & Biomolecular Chemistry

Cite this: *Org. Biomol. Chem.*, 2012, **10**, 6469

www.rsc.org/obc

COMMUNICATION

2-*O*-Alkylated *para*-benzamide α-helix mimetics: the role of scaffold curvature†

Valeria Azzarito,[a,b] Panchami Prabhakaran,[a,b] Alice I. Bartlett,[a,b] Natasha S. Murphy,[a,b] Michaele J. Hardie,[a] Colin A. Kilner,[a] Thomas A. Edwards,[b,c] Stuart L. Warriner[a,b] and Andrew J. Wilson*[a,b]

Received 16th May 2012, Accepted 3rd July 2012
DOI: 10.1039/c2ob26262b

The design and synthesis of a new 2-*O*-alklyated benzamide α-helix mimetic is described. Comparison with regioisomeric 3-*O*-alkylated benzamides permits a preliminary evaluation of the role that mimetic curvature has in determining molecular recognition properties.

The identification of ligands capable of modulating protein–protein interactions (PPIs) represents an area of significant focus.[1–3] PPIs fulfil myriad roles in biology and represent targets for therapeutic intervention. However, identification of competitive inhibitors is considered challenging; larger surfaces are involved at protein–protein interfaces alongside less well defined shapes and orientations of recognition handles[4] when compared with the conventional cavities that have been the traditional focus of medicinal chemistry.[5] One class of PPI that may be amenable to generic approaches of inhibitor design is the α-helix mediated PPI, in which a helical motif from one protein projects side chains into a cleft in its partner protein.[6] Chemoinformatic analyses reveal that these interactions can involve a range of different side chains but that interactions mediated by a single face (*e.g.* *i*, *i* + 4 (or 3) and *i* + 7 (or 8) residues) are more prevalent.[7] Several approaches have been described that exploit a common scaffold with appropriately positioned side chains to act as effective inhibitors of a range of target PPIs.[6,8,9] Mimicking an α-helix can be achieved with a constrained backbone mimetic,[10–14] helical foldamer[15–18] or a helix mimetic whereby a scaffold positions key functional motifs in an identical spatial orientation to those presented by the original α-helix.[19–34] Our group previously reported on the use of aromatic oligobenzamides as μM inhibitors of the p53/*h*DM2 interaction.[29,30] Herein we describe the design, characterisation and testing of a new α-helix mimetic based on a 2-*O*-alkylated template and compare it to the regioisomeric 3-*O*-alkylated benzamide analogue that we[30] and others studied previously.[24,31,35]

We performed molecular modelling on both scaffolds using isopropyl moieties as *O*-alkyl substituents (see ESI† for full details). Scaffolds were evaluated for α-helix mimicry by comparison with the p53 transactivation domain from the p53/*h*DM2 crystal structure (PDB ID: 1YCR)[36] in which three side chains – Phe19, Trp23 and Leu26 – are shown to play a key role at this interface (Fig. 1a). This PPI is a good model system given that it has served as a target for small molecule development.[37,38] Of the ensemble of structures within 1.5 kJ mol^{-1} of the lowest

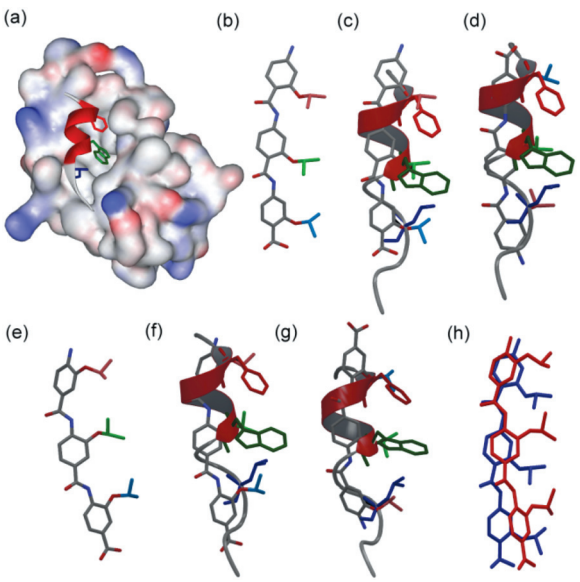

Fig. 1 Molecular modelling studies for helix mimetics **1** and **2**. (a) Structure of p53/*h*DM2 (PDB ID: 1YCR, Phe19 in red, Trp23 in green and Leu26 in blue). (b) Model of **1a**. (c) Overlay of **1a** with p53 (parallel, RMSD = 0.2170 (Å)). (d) Overlay of **1a** with p53 (antiparallel, RMSD = 0.2171). (e) Model of **2a**. (f) Overlay of **2a** with p53 (parallel, RMSD = 0.4951). (g) Overlay of **2a** with p53 (antiparallel, RMSD = 0.4953). (h) Overlay of **1a** (blue) with **2a** (red). Side chains in the mimetics are coloured (N to C terminus) to match the coding for p53.

[a]*School of Chemistry, University of Leeds, Woodhouse Lane, Leeds LS2 9JT, United Kingdom. E-mail: A.J.Wilson@leeds.ac.uk; Fax: +44 (0)113 3436565; Tel: +44 (0)113 3431409*
[b]*Astbury Centre for Structural Molecular Biology, University of Leeds, Woodhouse Lane, Leeds LS2 9JT, United Kingdom*
[c]*Institute of Molecular and Cellular Biology, University of Leeds, Woodhouse Lane, Leeds LS2 9JT, United Kingdom*

†Electronic supplementary information (ESI) available: Synthesis and characterisation, details of modelling, procedures for protein expression, purification and anisotropy. CCDC 870274 and 870275. For ESI and crystallographic data in CIF or other electronic format see DOI: 10.1039/c2ob26262b

energy conformation, several were observed to position side chains on one face, suggesting conformations mimicking the α-helix were accessible (Fig. 1b and e). Structures were aligned with the p53 helix and the root mean square deviation (RMSD) calculated on the basis of the agreement between the polypeptide and the scaffold with oxygen representing the α-carbon. Both scaffolds align with the p53 helix in parallel and anti-parallel orientations to the direction of the polypeptide chain (Fig. 1c–d and 1f–g and ESI, Fig. S27–S28†). Despite this, the backbone curvature is visibly different for both scaffolds (Fig. 1h). We attempted to quantify this effect by measuring differences in several key angles (*e.g.* the angle and pseudo-dihedrals between aromatic rings). However, no single measure accurately represents the curvature of the backbone and relates it to the presentation of individual side chains in a meaningful manner as the different hydrogen-bonded geometries in scaffolds **1** and **2** impose constraints on both the backbone curvature and the twist around the Ar–amide axes.

We were intrigued to determine whether these subtle variations in backbone architecture and side chain presentation would manifest a difference in binding affinity to target proteins. Following the modelling studies we synthesised a series of mimetics (Fig. 2) using minor variations to the method described previously (see ESI, Schemes S1 and S2†).[39] Compounds **1a** and **2a** incorporated isopropyl side chains for structural studies, whereas **1b** and **2b–c** incorporated benzyl, 2-methylnapthyl and isopropyl side chains in both orientations to provide side chains mimicking those present in the p53 transactivation domain (Fig. 2). We were unable to obtain the reversed sequence of **1b** *i.e.* **1c** because the precursors were not sufficiently soluble to permit the last 2 steps of the synthesis.

Structural studies of the conformational properties of both **1a** and **2a** including VT NMR, dilution and H/D exchange (see ESI†) indicate strong S(6) for **1a** and S(5) for **2a** intramolecular hydrogen bonding between the amide NH and the alkoxy oxygen atom. In both cases, the NH at the N terminus exchanges slower than the NH at the carboxy terminus of both **1a** and **2a** whilst the amide protons of **1a** (S(6) hydrogen bonding) exchange an order of magnitude slower than **2a** (S(5) hydrogen bonding) implying stronger hydrogen-bonding for **1a** in line with our work on model compounds.[40] Taken together these data indicate **1a** adopts an extended conformation in which rotation around the Ar–CO axes is restricted by S(6) intramolecular hydrogen bonding which contrasts with our studies on **2a** in which rotation around the Ar–NH axes is restricted by S(5) intramolecular hydrogen bonding.[30,39] 2D ^{1}H–^{1}H NOESY experiments on **1a** (see ESI, Fig. S7†) and **2a**,[30,39] provide confirmation of this behaviour. Crystallographic analyses support the solution observations and provide additional information. The crystal structure of the nitro-ester analogue of trimer **2a** (**3a**, Fig. 3a) places two side chains on the same face with the side chain at the N-terminus on the opposite face and confirms the presence of S(5) intramolecular hydrogen bonding. We also obtained a structure of a synthetic intermediate, dimer **4a** (Fig. 3b) on route to **1a**. The structure places the isopropyl side chains on opposing faces and confirms the presence of S(6) intramolecular hydrogen bonding. In support of the modelling studies, the curvature of **3a** and **4a** is visibly different (Fig. 3c and ESI, Fig. S29† for a more detailed analysis). The different curvature in **3a** relative to **4a** arises because the placement of the *O*-alkyl group in the 2-position allows 6-membered hydrogen-bonding with minimal distortion of the idealized backbone geometry. In contrast, for **3a** 5-membered hydrogen-bonding "bends" the backbone and imposes different twisting around the Ar–amide axes. Notably – these analyses suggest the nitro and amino terminal groups have little influence on the oligomer conformation.

We tested the compounds against the p53/*h*DM2 interaction using fluorescence anisotropy (FA) displacement (Table 1 and Fig. S30†). Low potency was observed for **1a** possessing isopropyl side chains, consistent with our earlier results for **2a**,[30] whereas for **1b** possessing side chains that mimic those present on the p53 helix, single digit μM IC_{50} values were obtained. All derivatives with side chains matched to the p53 sequence gave low IC_{50}'s in the assay (see ESI† for full details).

To evaluate the role of helix mimetic curvature on binding affinity we compared the results for **2b** against **1b**. The results

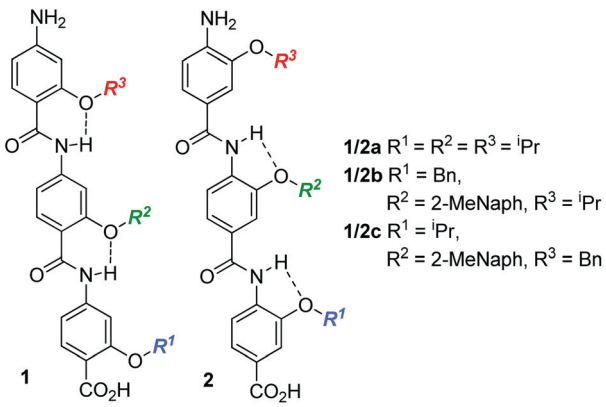

Fig. 2 Structures of compounds **1a–b**, **2a**,[30] **2b** and **2c**.[30]

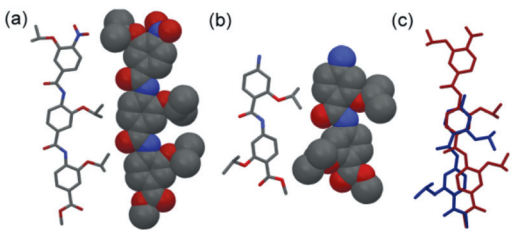

Fig. 3 (a) Solid state structure of **3a**. (b) Solid state structure of **4a**. (c) Superimposition of **3a** and **4a** (RMSD = 0.2436).

Table 1 IC_{50} values obtained from fitting the FA displacement assay

Compound	IC_{50}
$p53_{15–31}$	1.35 ± 0.09 μM
1a	35.2 ± 7.5 μM
1b	4.80 ± 0.43 μM
2a	25.5 ± 6.3 μM
2b	6.35 ± 0.30 μM
2c	4.15 ± 0.20 μM

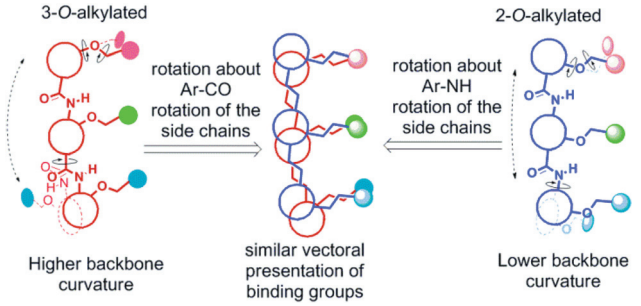

Fig. 4 Schematic depicting rotatable bonds (one amide and one alkoxy is highlighted for each scaffold) in regioisomeric helix mimetics. Rotation about bonds (black arrows) gives rise to multiple pharmacophores some of which are similarly productive for helix mimicry.

show that the two scaffolds give rather similar activities in this assay suggesting backbone curvature does not play a major role in determining the binding affinity towards the *h*DM2 cleft. Whilst helical curvature maybe useful in understanding the properties of biological macromolecules,[41] direct translation of this concept to helical mimics[19,24] requires a more detailed understanding of the complex conformational space available to such molecules in which the subtle interplay of backbone and side chain torsional angles can self-compensate to enable the dynamic construction of a variety of pharmacophores. Helix mimetics are often represented as linear oligomers with side chains on one face and mimicry evaluated on the basis of side chain distances for a single conformation. For the series of helix mimetics described here, despite different backbone curvature, free rotation around Ar–NH/CO axes coupled with rotations in the alkoxy side chains are likely to allow side chains to be presented along similar vectors for effective biological mimicry (Fig. 4).

Conclusions

In summary, we have described the design, synthesis and structural studies of a new α-helix mimetic scaffold, illustrating that helix mimetic curvature can be readily tuned by subtle placement of side-chain mimicking groups. Preliminary evaluation of this new scaffold revealed minimal differences in potency for antagonism of the p53/*h*DM2 interaction, highlighting the complex relationship between helix mimetic conformation and molecular recognition whilst suggesting strict geometrical matching of side chain presentation by proteomimetic scaffolds is not essential for effective inhibition of PPIs.

Acknowledgements

This work was supported by the European Research Council [ERC-StG-240324], NSM acknowledges the University of Leeds for the award of a Mary & Alice Smith PhD Scholarship. Crystallographic assistance of Dr Amber L. Thompson, Oxford University is gratefully acknowledged.

Notes and references

1 A. J. Wilson, *Chem. Soc. Rev.*, 2009, **38**, 3289–3300.
2 J. A. Wells and C. L. McLendon, *Nature*, 2007, **450**, 1001–1009.
3 H. Yin and A. D. Hamilton, *Angew. Chem., Int. Ed.*, 2005, **44**, 4130–4163.
4 O. Keskin, A. Gursoy, B. Ma and R. Nussinov, *Chem. Rev.*, 2008, **108**, 1225–1244.
5 R. E. Babine and S. L. Bender, *Chem. Rev.*, 1997, **97**, 1359–1472.
6 T. Edwards and A. Wilson, *Amino Acids*, 2011, **41**, 743–754.
7 B. N. Bullock, A. L. Jochim and P. S. Arora, *J. Am. Chem. Soc.*, 2011, **133**, 14220–14223.
8 C. G. Cummings and A. D. Hamilton, *Curr. Opin. Chem. Biol.*, 2010, **14**, 341–346.
9 J. M. Davis, L. K. Tsou and A. D. Hamilton, *Chem. Soc. Rev.*, 2007, **36**, 326–334.
10 A. Patgiri, K. K. Yadav, P. S. Arora and D. Bar-Sagi, *Nat. Chem. Biol.*, 2011, **7**, 585–587.
11 L. K. Henchey, S. Kushal, R. Dubey, R. N. Chapman, B. Z. Olenyuk and P. S. Arora, *J. Am. Chem. Soc.*, 2010, **132**, 941–943.
12 R. E. Moellering, M. Cornejo, T. N. Davis, C. D. Bianco, J. C. Aster, S. C. Blacklow, A. L. Kung, D. G. Gilliland, G. L. Verdine and J. E. Bradner, *Nature*, 2009, **462**, 182–188.
13 G. H. Bird, N. Madani, A. F. Perry, A. M. Princiotto, J. G. Supko, X. He, E. Gavathiotis, J. G. Sodroski and L. D. Walensky, *Proc. Natl. Acad. Sci. U. S. A.*, 2010, **107**, 14093–14098.
14 R. S. Harrison, N. E. Shepherd, H. N. Hoang, G. Ruiz-Gómez, T. A. Hill, R. W. Driver, V. S. Desai, P. R. Young, G. Abbenante and D. P. Fairlie, *Proc. Natl. Acad. Sci. U. S. A.*, 2010, **107**, 11686–11691.
15 W. S. Horne, L. M. Johnson, T. J. Ketas, P. J. Klasse, M. Lu, J. P. Moore and S. H. Gellman, *Proc. Natl. Acad. Sci. U. S. A.*, 2009, **106**, 14751–14756.
16 W. S. Horne, M. D. Boersma, M. A. Windsor and S. H. Gellman, *Angew. Chem., Int. Ed.*, 2008, **47**, 2853–2856.
17 A. D. Bautista, J. S. Appelbaum, C. J. Craig, J. Michel and A. Schepartz, *J. Am. Chem. Soc.*, 2010, **132**, 2904–2906.
18 E. A. Harker, D. S. Daniels, D. A. Guarracino and A. Schepartz, *Bioorg. Med. Chem.*, 2009, **17**, 2038–2046.
19 J. L. Yap, X. Cao, K. Vanommeslaeghe, K.-Y. Jung, C. Peddaboina, P. T. Wilder, A. Nan, A. D. MacKerell, W. R. Smythe and S. Fletcher, *Org. Biomol. Chem.*, 2012, **10**, 2928–2933.
20 M. J. Adler and A. D. Hamilton, *J. Org. Chem.*, 2011, **76**, 7040–7047.
21 I. Saraogi, J. A. Hebda, J. Becerril, L. A. Estroff, A. D. Miranker and A. D. Hamilton, *Angew. Chem., Int. Ed.*, 2010, **49**, 736–739.
22 J. M. Rodriguez, N. T. Ross, W. P. Katt, D. Dhar, G.-I. Lee and A. D. Hamilton, *ChemMedChem*, 2009, **4**, 649–656.
23 J. M. Rodriguez, L. Nevola, N. T. Ross, G.-I. Lee and A. D. Hamilton, *ChemBioChem*, 2009, **10**, 829–833.
24 I. Saraogi, C. D. Incarvito and A. D. Hamilton, *Angew. Chem., Int. Ed.*, 2008, **47**, 9691–9694.
25 J. M. Rodriguez and A. D. Hamilton, *Angew. Chem., Int. Ed.*, 2007, **46**, 8614–8617.
26 H. Yin, G.-I. Lee, K. A. Sedey, J. M. Rodriguez, H.-G. Wang, S. M. Sebti and A. D. Hamilton, *J. Am. Chem. Soc.*, 2005, **127**, 5463–5468.
27 H. Yin, G.-I. Lee, K. A. Sedey, O. Kutzki, H. S. Park, B. P. Orner, J. T. Ernst, H.-G. Wang, S. M. Sebti and A. D. Hamilton, *J. Am. Chem. Soc.*, 2005, **127**, 10191–10196.
28 H. Yin, G.-I. Lee, H. S. Park, G. A. Payne, J. M. Rodriguez, S. M. Sebti and A. D. Hamilton, *Angew. Chem., Int. Ed.*, 2005, **44**, 2704–2707.
29 F. Campbell, J. P. Plante, T. A. Edwards, S. L. Warriner and A. J. Wilson, *Org. Biomol. Chem.*, 2010, **8**, 2344–2351.
30 J. P. Plante, T. Burnley, B. Malkova, M. E. Webb, S. L. Warriner, T. A. Edwards and A. J. Wilson, *Chem. Commun.*, 2009, 5091–5093.
31 A. Shaginian, L. R. Whitby, S. Hong, I. Hwang, B. Farooqi, M. Searcey, J. Chen, P. K. Vogt and D. L. Boger, *J. Am. Chem. Soc.*, 2009, **131**, 5564–5572.
32 S. Marimganti, M. N. Cheemala and J.-M. Ahn, *Org. Lett.*, 2009, **11**, 4418–4421.
33 S. M. Biros, L. Moisan, E. Mann, A. Carella, D. Zhai, J. C. Reed and J. Rebek, *Bioorg. Med. Chem. Lett.*, 2007, **17**, 4641–4645.
34 J. T. Ernst, J. Becerril, H. S. Park, H. Yin and A. D. Hamilton, *Angew. Chem., Int. Ed.*, 2003, **42**, 535–539.
35 T.-K. Lee and J.-M. Ahn, *ACS Comb. Sci.*, 2010, **13**, 107–111.

36 P. H. Kussie, S. Gorina, V. Marechal, B. Elenbaas, J. Moreau, A. J. Levine and N. P. Pavletich, *Science*, 1996, **274**, 948–953.
37 L. T. Vassilev, B. T. Vu, B. Graves, D. Carvajal, F. Podlaski, Z. Filipovic, N. Kong, U. Kammlott, C. Lukacs, C. Klein, N. Fotouhi and E. A. Liu, *Science*, 2004, **303**, 844–848.
38 S. Shangary, D. Qin, D. McEachern, M. Liu, R. S. Miller, S. Qiu, Z. Nikolovska-Coleska, K. Ding, G. Wang, J. Chen, D. Bernard, J. Zhang, Y. Lu, Q. Gu, R. B. Shah, K. J. Pienta, X. Ling, S. Kang, M. Guo, Y. Sun, D. Yang and S. Wang, *Proc. Natl. Acad. Sci. U. S. A.*, 2008, **105**, 3933–3938.
39 J. Plante, F. Campbell, B. Malkova, C. Kilner, S. L. Warriner and A. J. Wilson, *Org. Biomol. Chem.*, 2008, **6**, 138–146.
40 P. Prabhakaran, V. Azzarito, T. Jacobs, M. J. Hardie, C. A. Kilner, T. A. Edwards, S. L. Warriner and A. J. Wilson, *Tetrahedron*, 2012, **68**, 4485–4491.
41 D. J. Barlow and J. M. Thornton, *J. Mol. Biol.*, 1988, **201**, 601–619.

